Quantitative Structure−Activity Relationship of Sesquiterpene Lactones as Inhibitors of the Transcription Factor NF-κB

Bettina Siedle,[†] Alfonso J. García-Piñeres,[†] Renato Murillo,[§] Jürgen Schulte-Mönting,[∥] Victor Castro,[§] Peter Rüngeler,[†] Christoph A. Klaas,[†] Fernando B. Da Costa,[⊥] Wanda Kisiel,[‡] and Irmgard Merfort[†,*]

Institut für Pharmazeutische Wissenschaften, Lehrstuhl für Pharmazeutische Biologie, Universität Freiburg, 79104 Freiburg, Germany, Escuela de Quimica y CIPRONA, Universidad de Costa Rica, San José, Costa Rica, Faculdade de Ciências Farmacêuticas de Ribeirão Preto, Universidade de São Paulo, Brazil, Institut für Medizinische Biometrie und Medizinische Informatik, Universität Freiburg, 79104 Germany, and Department of Phytochemistry, Institute of Pharmacology, Polish Academy of Sciences, 31-343 Kraków, Poland

Received January 22, 2004

Sesquiterpene lactones (SLs) are the active compounds of a variety of tradionally used medicinal plants from the Asteraceae family. They are known to possess a considerable antiinflammatory activity in different inflammation models. They inhibit the transcription factor NF-κB probably by alkylating cysteine38 in the DNA binding domain of the p65 subunit. Here we investigate a set of 103 different sesquiterpene lactones representing 6 structural groups (44 germacranolides, 16 heliangolides, 22 guaianolides, 9 pseudoguaianolides, 2 hypocretenolides, 10 eudesmanolides) for their NF-κB inhibiting properties and the resulting IC_{100}-values were submitted to a QSAR study. Properties important for the inhibition potency are discussed for the whole data set and for subsets of the different structural classes.

Introduction

Sesquiterpene lactones (SLs) have been isolated from numerous genera of the Asteraceae family. They are described as the active constituents of a variety of medicinal plants used in traditional medicine for the treatment of inflammatory diseases. Various studies have investigated how these natural compounds exert their antiinflammatory effect. SLs modulate many inflammatory processes, such as the exocytosis of cathepsin G and acid phosphatase from the azurophilic granules of rat polymorphonuclear leukocytes, the release of histamine from mast cells and serotonine from blood platelets, and the exocytosis of elastase from human neutrophils.[1−5] They inhibit the 5-lipoxygenase and leukotriene C4 synthase in human blood cells.[6] SLs possess pro-apoptotic effects which can be desirable in eliminating nonfunctional cells in inflammatory tissues.[7] In vivo their antiinflammatory activity was proven in the rat paw and mouse ear edema.[2,5] Most importantly, we and others have recently demonstrated that SLs inhibit the central transcription factor NF-κB.[8−11] Additionally, we could show that also DNA binding of the transcription factors nuclear factor of activated T-cells (NFAT) and activator protein 1 (AP-1) was prevented.[12] These transcription factors play a pivotal role in controlling the expression of multiple inflammatory and immune genes involved in toxic shock, asthma, rheumatoid arthritis, or cancer.[13,14]

Thus, NF-κB promotes the expression of over 150 target genes in response to inflammatory stimulators, such as interleukin-1, -2, and -6 or TNF-α, as well as genes encoding immunoreceptors, cell adhesion molecules, and enzymes such as cyclooxygenase-II and iNOS.[15,16] NF-κB is composed most frequently of a p50 and a p65 subunit and is retained in the cytoplasm bound to its inhibitory subunit IκB in its inactive form. Inducers of NF-κB such as bacterial lipopolysaccharides or inflammatory cytokines release active NF-κB from the cytoplasmic complex by activating the IκB−kinase complex (IKK), which phosphorylates IκB. This is a marker for subsequent ubiquitinylation and degradation of the inhibitory subunit. Free NF-κB dimer translocates into the nucleus where it stimulates the transcription of its target genes.[16] Because of its central role in regulating inflammatory responses, a pharmacological inhibition of NF-κB activation in vivo could be beneficial in the treatment of inflammation.[17]

Previously, we could provide evidence that SLs, such as parthenolide and helenalin, inhibit DNA binding of NF-κB in cell cultures most probably by alkylating p65 at Cys38 and that the p50 subunit is not modified. Although a slight inhibition of IκB degradation by SLs was also detected, we determined that this effect is secondary to the alkylation of p65.[8,18,19] There are strong indications that this is a general mechanism for SLs, which possess α,β- or α,β,γ-unsaturated carbonyl structures such as α-methylene-γ-lactones or α,β-unsaturated cyclopentenones. These structural elements preferably react with nucleophiles, especially sulfhydryl groups by a Michael-type addition.[20,21]

Preliminary quantitative structure−activity relationships (QSAR) undertaken with a selection of 28 SLs of all major skeletal classes revealed that a strong NF-κB inhibitory activity correlates with the number of alkylating centers, such as the methylene lactone and conjugated keto or aldehyde functions, but not conju-

* To whom correspondence should be addressed: Stefan-Meier-Str. 19. Phone: +49-761-2038373. Fax: +49-761-2038383. E-mail: irmgard.merfort@pharmazie.uni-freiburg.de.
[†] Institut für Pharmazeutische Wissenschaften, Universität Freiburg.
[§] Universidad de Costa Rica.
[⊥] Universidade de São Paulo.
[∥] Institut für Medizinische Biometrie und Medizinische Informatik, Universität Freiburg.
[‡] Polish Academy of Sciences.

10.1021/jm049937r CCC: $27.50
Published on Web 10/19/2004

gated ester groups. Lipophilicity did not influence NF-κB inhibitory activity in this set of compounds.[9]

To establish a QSAR model for a larger set of SLs with a wider structural diversity, we here investigate a total of 103 different sesquiterpene lactones representing 6 structural groups for their NF-κB inhibiting properties: 44 germacranolides, such as germacrolides, melampolides and 4,5-dihydrogermacranolides, 16 furanoheliangolides, 22 guaianolides, 9 pseudoguaianolides, 2 hypocretenolides, and 10 eudesmanolides. The resulting micromolar concentrations which completely inhibit NF-κB DNA binding and which are described as IC_{100} values were submitted to a QSAR study. We enlarged the number of the descriptors to study whether further properties of the SLs, e.g. the molecular geometry or the chemical environment may influence the NF-κB inhibitory activity. Our QSAR studies could contribute in the search for a lead structure which can be optimized for the development of a pharmaceutically used antiinflammatory cytokine suppressing remedy.

Results

NF-κB Inhibitory Activity of Sesquiterpene Lactones. Electrophoretic mobility shift assay (EMSA) has become the method of choice to analyze the binding of transcription factors to the DNA and therefore to study the influence of substances on this interaction. The strength of DNA binding is proportional to the intensity of the specific NF-κB band, and the inhibitory activity of a compound can be deduced from the band intensity obtained after treating cells with the respective compound. Up to now, we have studied 48 different SLs on their antiinflammatory activity using the transcription factor NF-κB as molecular target.[5,9,39,42,45,55,62] In this study, we summarize our previous results of NF-κB DNA inhibiting properties and investigated further 57 SLs (for detailed references see Table 5). Jurkat T cells were incubated with the respective SL at various concentrations for 1 h and subsequently stimulated with TNF-α for 1 h. Total protein extracts were prepared and analyzed for NF-κB DNA binding in an EMSA (for example, see Figure 1). At first 10, 20, 50, and 100 μM concentrations of the SL were studied. Depending on the activity of the compound either lower concentrations, such as 1, 2.5, and 5 μM or higher concentrations, such as 200 and 300 μM were subsequently investigated. The concentration of the respective SL which completely prevented NF-κB DNA binding was named as IC_{100} value (see Table 5 in which all published and new IC_{100} values are listed).

Structure−Activity Relationships. A 3D-structure was created for all investigated SLs using the HYPERCHEM program. The low energy conformations were semiempirically minimized using the AM1 algorithm and transferred into the CAChe database. The calculated descriptors (see Table 4) were checked for intercorrelation in a correlation matrix. Intercorrelation ($r^2 > 0.65$) could be detected between molar refractivity and topological parameters as well as among the topological parameters themselves. The monoparametric regression of the descriptors with the pIC_{100} value was extracted from the matrix. A low statistically significant monoparametric regression could be obtained for all parameters used. The best monoparametric regression arises by correlating the pIC_{100} and the number of α,β-unsaturated carbonyl functions in the molecule ($r = 0.683$) followed by the correlation of pIC_{100} and LUMO-2 ($r = 0.650$), electron affinity ($r = 0.630$), and LUMO-1 ($r = 0.629$), respectively.

Multiple Linear Regression with the Entire Dataset of 103 SLs Including All Major Skeletal Classes. Using the two-step model selection procedure (decribed in Materials and Methods) an equation with four variables proved to be the best to describe the correlation between the inhibition of NF-κB DNA binding activity and the physicochemical properties of the molecules.

$$pIC_{100} = 0.239\ (\pm 0.054)\ \mathrm{UNC} + 0.431\ (\pm 0.164)\ \mathrm{ML} + 0.648\ (\pm 0.143)\ \mathrm{EA} + 0.050\ (\pm 0.023)\ \mathrm{SH3} - 2.861\ (\pm 0.169)$$

$$n = 103,\ R = 0.772,\ R^2 = 0.596,\ s = 0.381,\ F = 36.2,\ P < 0.0001 \quad (1)$$

The most important variables for the biological activity turned out to be the number of α,β-unsaturated carbonyl functions confirming the results from Rüngeler et al. who used a smaller dataset of 28 SLs.[9] Additionally, the existence of an α-methylene-γ-lactone moiety is a very important criterion, which has already been described as a significant feature for various biological activities of SLs.[2,3,9,22] Electron affinity, coding for the change of a molecule's total energy when an electron is taken up and representing the reactivity of a molecule, e.g., toward biological nucleophiles, and the topological parameter shape 3 which quantifies the molecule's centrality of branching are further important descriptors.

In classical QSAR analyses, substances possessing the same skeletal type are compared. Thus, SLs were classified according to their major skeletal classes, and the multiple linear regression analysis was repeated with smaller subsets of SLs. According to their biosynthesis the 103 SLs were divided into the germacranolides with a 10-membered ring system, the guaianolides and pseudoguaianolides with a 7- and 5-membered ring system and the eudesmanolides with two 6-membered rings (see Figures 5−10).[23] Among the germacranolides the heliangolides serve special interest because their flexible 10-membered ring system is bridged by an oxygen function that makes it more rigid.

Multiple Linear Regression with Germacranolides. The germacranolides (60 compounds) were the largest group among the investigated SLs (for structures see Figure 5 and Figure 6). A QSAR equation with three descriptors was found as the best solution to describe the correlation between NF-κB inhibitory activity and the available parameters. Further equations with more descriptors did not provide statistically significant improvements.

$$pIC_{100} = 0.271\ (\pm 0.068)\ \mathrm{UNC} + 0.452\ (\pm 0.226)\ \mathrm{ML} + 0.518\ (\pm 0.163)\ \mathrm{EA} - 2.597\ (\pm 0.224)$$

$$n = 60,\ R = 0.779,\ R^2 = 0.607,\ s = 0.329,\ F = 28.8,\ P < 0.0001 \quad (2)$$

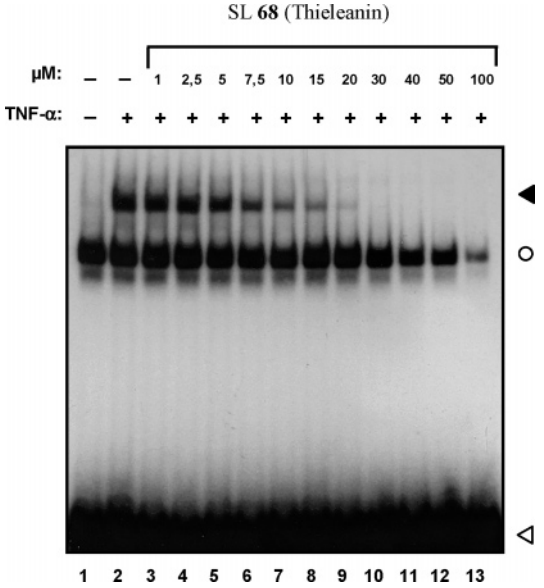

Figure 1. The effect of SL **68** on NF-κB DNA binding. Lane 1 shows unstimulated control cells, in lane 2, cells were treated with 200 U/mL TNF-α alone. In lanes 3−13 cells were pretreated for 1 h with various concentrations of compound **68** and subsequently stimulated with TNF-α for 1 h. A filled arrowhead indicates the position of NF-κB DNA complexes. The open circle denotes a nonspecific activity binding to the probe. The open arrowhead shows unbound oligonucleotide.

The same parameters as in eq 1 occur in eq 2, except for shape 3. Again, the number of unsaturated carbonyl functions in the molecule, the existence of an α-methylene-γ-lactone, and the electron affinity were the most important features for the inhibitory activity of the flexible germacranolides. Topological parameters describing the shape of the molecule were not found to be significant.

Regarding the errors of the calculated IC_{100} values, it was obvious that representatives from the group of heliangolides were most often poorly described by eq 2. Therefore, we separated the heliangolides and defined them as an own subgroup.

The two-step model selection procedure was carried out with the remaining 44 germacranolides and two eqs 3a and 3b were obtained. These only differed in one variable with slight impairment of the statistical parameters in eq 3b.

$$pIC_{100} = 1.001\ (\pm 0.256)\ ML + 0.327\ (\pm 0.082)\ UNA + 0.977\ (\pm 0.162)\ EA - 2.913\ (\pm 0.261)$$

$$n = 44,\ R = 0.848,\ R^2 = 0.718,\ s = 0.251,\ F = 34.0,\ P < 0.0001 \quad (3a)$$

$$pIC_{100} = 0.239\ (\pm 0.061)\ UNC + 0.913\ (\pm 0.262)\ ML + 0.599\ (\pm 0.218)\ EA - 2.983\ (\pm 0.262)$$

$$n = 44,\ R = 0.846,\ R^2 = 0.715,\ s = 0.252,\ F = 33.5,\ P < 0.0001 \quad (3b)$$

Compared to eq 2, considering all germacranolides, a visible improvement of the statistical parameters was obtained and the correlation coefficient was improved (R = 0.848 or 0.846 compared to R = 0.779 (see also Figure 2). Interestingly, the descriptors were the same in eqs 3b and 2, but changed in eq 3a in which the parameter "existence of α,β-unsaturated acyl residues" (UNA) appeared. This contrasts previous investigations where this variable did not significantly contribute to the correlation.[9]

When comparing the experimental with the predicted IC_{100} values, there is good agreement over a wide range, but there are also seven SLs with major deviations (**4**, **14**, **19**, **22**, **30**, **38**, and **43**) to be observed. For some of these SLs a possible explanation may be given: e.g., 7-hydroxycostunolide (**38**) has only one α,β-unsaturated structural element in the form of an α-methylene-γ-lactone group, but shows remarkable activity in the test system. However, close to the α-methylene-γ-lactone a hydroxy group is situated which could stabilize a covalent reaction by forming hydrogen bonds to the NF-κB protein. This possible phenomenon is not considered in eqs 3a and 3b and could therefore result in the worse prediction of SL **38**'s activity. For SLs **30** and **43**, a lower IC_{50} value is predicted, which could be due to the semiquantitative measuring method, where concentrations of 5, 10, 20, 50, 100, and 200 μM were used. All substances with an inhibitory concentration lying between two of these standard values will be assigned to the higher concentration.

Table 1. Experimental and Calculated IC_{100} and pIC_{100} Values for the Dataset of 44 Germacranolides without Furanoheliangolides, Calculations Were Obtained by eqs 3a and 3b

No. SL	IC_{100} exp	IC_{100} calcd (3a)	IC_{100} calcd (3b)	pIC_{100} exp	pIC_{100} calcd (3a)	pIC_{100} calcd (3b)
1	12.5	11.96	12.04	−1.097	−1.078	−1.080
2	12.5	14.64	13.63	−1.097	−1.166	−1.134
3	12.5	16.72	14.78	−1.097	−1.223	−1.170
4	100	39.31	43.28	−2.000	−1.594	−1.636
5	12.5	13.78	13.13	−1.097	−1.139	−1.118
6	25	22.55	17.76	−1.097	−1.353	−1.249
7	25	18.09	15.51	−1.398	−1.257	−1.191
8	12.5	18.17	15.55	−1.097	−1.259	−1.192
9	5	10.36	10.09	−0.699	−1.015	−1.004
10	10	7.07	7.98	−1.000	−0.849	−0.902
11	5	5.68	6.98	−0.699	−0.755	−0.844
12	5	6.43	7.53	−0.699	−0.808	−0.877
13	10	5.56	6.88	−1.000	−0.745	−0.838
14	5	15.12	12.72	−0.699	−1.180	−1.104
15	10	9.84	9.77	−1.000	−0.993	−0.990
16	10	8.29	8.80	−1.000	−0.919	−0.944
17	5	11.24	10.60	−0.699	−1.051	−1.025
18	5	10.27	10.03	−1.000	−1.012	−1.001
19	50	8.85	9.16	−1.301	−0.947	−0.962
20	10	10.55	10.20	−1.000	−1.023	−1.009
21	5	7.38	8.19	−0.699	−0.868	−0.913
22	200	46.53	48.00	−2.000	−1.668	−1.681
23	50	64.62	58.71	−1.699	−1.810	−1.769
24	50	28.49	20.50	−1.699	−1.455	−1.312
25	20	47.16	48.40	−1.301	−1.674	−1.685
26	50	34.97	40.29	−1.699	−1.544	−1.605
27	50	52.42	51.64	−1.699	−1.720	−1.713
28	50	38.43	42.69	−1.699	−1.585	−1.630
29	50	55.83	53.67	−1.699	−1.747	−1.730
30	50	16.88	23.59	−1.699	−1.227	−1.373
31	50	52.42	51.64	−1.699	−1.720	−1.713
32	100	72.15	62.81	−2.000	−1.858	−1.798
33	50	20.39	26.49	−1.301	−1.309	−1.423
34	20	14.13	21.16	−1.301	−1.150	−1.325
35	300	300.09	299.81	−2.477	−2.477	−2.477
36	50	56.34	53.97	−1.699	−1.751	−1.732
37	50	74.80	64.22	−1.699	−1.874	−1.808
38	10	33.66	39.35	−1.000	−1.527	−1.595
39	20	17.27	23.92	−1.000	−1.237	−1.379
40	10	20.61	16.80	−1.000	−1.314	−1.225
41	10	7.08	4.61	−1.000	−0.850	−0.664
42	10	7.41	4.74	−1.000	−0.870	−0.676
43	200	50.91	50.72	−2.301	−1.707	−1.705
44	10	7.21	8.82	−1.000	−0.858	−0.946

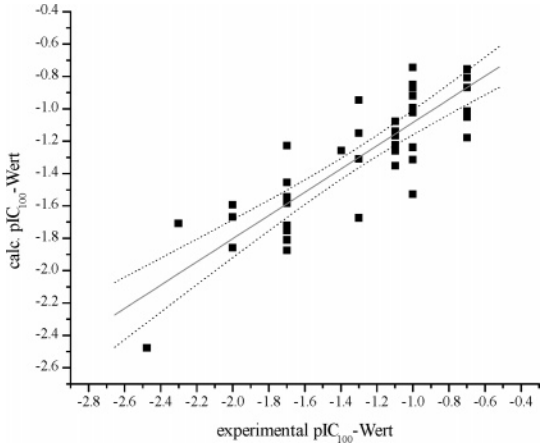

Figure 2. Regression model of eq 3a derived from germacranolides without furanoheliangolides ($n = 44$). Data points, regression line and 95% confidenc interval (pointed).

Table 2. Experimental and Calculated IC_{100} and pIC_{100} Values for the Dataset of 16 Furanoheliangolides. Equation 4 Was Used for Calculation

No. SL	IC_{100} exp	IC_{100} calcd	pIC_{100} exp	pIC_{100} calcd
45	50	14.16	−1.000	−1.151
46	200	62.06	−2.301	−1.793
47	200	162.54	−2.301	−2.211
48	5	4.59	−0.699	−0.662
49	20	12.73	−1.301	−1.105
50	10	22.95	−1.000	−1.361
51	5	5.41	−0.699	−0.733
52	100	111.30	−2.000	−2.047
53	5	4.64	−0.699	−0.666
54	2.5−5	3.00	−0.398	−0.477
55	5	3.00	−0.699	−0.477
56	200	175.36	−2.301	−2.244
57	10	8.11	−1.000	−0.909
58	5	4.59	−0.699	−0.662
59	10	34.43	−1.000	−1.537
60	10	12.42	−1.000	−1.094

A calculation of a new QSAR analysis excluding these seven SLs (eq 3c), resulted in an increase of the correlation coefficient ($R = 0.901$) with the same descriptors as in eq 3a.

$$pIC_{100} = 1.012\ (\pm 0.206)\ ML + 0.347\ (\pm 0.071)\ UNA + 0.933\ (\pm 0.134)\ EA - 2.893\ (\pm 0.210)$$

$$n = 37,\ R = 0.904,\ R^2 = 0.812,\ s = 0.201,\ F = 49.06,\ P < 0.0001 \quad (3c)$$

Regarding the group of 16 heliangolides, a significant equation was obtained with three describing parameters:

$$pIC_{100} = 1.060\ (\pm 0.141)\ ENONE + 0.731\ (\pm 0.126)\ SH2 - 0.628\ (\pm 0.132)\ ATOM - 3.462\ (\pm 1.101)$$

$$n = 16,\ R = 0.933,\ R^2 = 0.870,\ s = 0.233,\ F = 26.8,\ P < 0.0001 \quad (4)$$

In this subgroup the presence of further conjugated keto or aldehyde functions in the ring is more important than the existence of the α-methylene-γ-lactone function. Two examples would be SLs **52** and **53**. Both compounds lack a methylene lactone, but inhibit NF-κB DNA binding. Other important parameters are the topological parameter shape2, which increases the activity, and the number of oxygen atoms, which diminishes the biological activity.

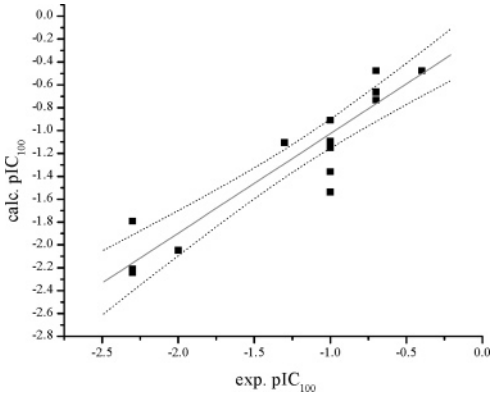

Figure 3. Regression model of eq 4 derived from furanoheliangolides ($n = 16$). Data points, regression line and 95% confidence interval (pointed).

The correlation coefficient, which was calculated from eq 4 and which describes the furanoheliangolide's activity, is very high ($R = 0.933$) (see Figure 3 and Table 2). However, it has to be considered that the data set of 16 compounds is low, so that these results probably have a preliminary character.

Multiple Linear Regression with Guaianolides. The group of guaianolides consists of 22 members (for structures, see Figure 7) and was also investigated in the QSAR analysis. The following QSAR equation with four describing parameters was derived:

$$pIC_{100} = 0.303\ (\pm 0.088)\ UNC + 0.639\ (\pm 0.174)\ CN2 - 0.109\ (\pm 0.027)\ MR - 0.346\ (\pm 0.114)\ OH + 0.053\ (\pm 0.577)$$

$$n = 22,\ R = 0.818,\ R^2 = 0.669,\ s = 0.282,\ F = 8.58,\ P = 0.0006 \quad (5)$$

As in eqs 1, 2, and 3b, the number of unsaturated α,β-carbonyl functions is also a very important descriptor for guaianolides. The α-methylene-γ-lactone group has not been considered, because all investigated guaianolides possess this structural element. The number of free hydroxyl groups in the molecule is more important. An increasing number decreases the biological activity. Accordingly, acetylation of SL **62** to **61** strongly increases its inhibitory activity. Interestingly, two topological descriptors, connectivity2 and the molar refraction index. also contribute to the activity of the guaianolides. The molar refractivity index is a composite of refractive index, density, and molecular weight and is closely related to polarizability of a molecule. Therefore, it is coding for the tendency of its electron sheath to react to changes of the surrounding charge. The molecular connectivity $^2\chi$ index encodes in a particular manner the structural information resident in the molecular skeleton.[24] The contribution of topological parameters to the inhibitory activity may be explained by the relative rigid structure of guaianolides.

As with the previous subgroups. the separate examination of the guaianolides also results in an amelioration of the statistical parameters for the calculated equations and in a better correlation coefficient of $R = 0.818$.

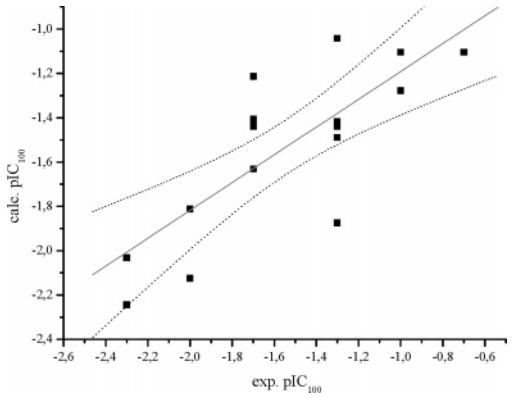

Figure 4. Regression model of eq 5 derived from guaianolides (n = 16). Data points, regression line and 95% confidence interval (pointed).

Table 3. Experimental and Calculated IC_{100} and pIC_{100} Values for the Dataset of 22 Guaianolides. Equation 5 Was Used for Calculations

No. SL	IC_{100} exp	IC_{100} calcd	pIC_{100} exp	pIC_{100} calcd
61	20	74.8	−1.301	−1.874
62	100	133.3	−2.000	−2.125
63	50	16.4	−1.699	−1.214
64	20	30.8	−1.301	−1.489
65	5	5.7	−0.699	−0.757
66	20	24.3	−1.301	−1.386
67	20	24.3	−1.301	−1.386
68	20	26.9	−1.301	−1.429
69	50	25.4	−1.699	−1.406
70	20	26.2	−1.301	−1.418
71	5	12.7	−0.699	−1.105
72	10	12.7	−1.000	−1.105
73	50	26.9	−1.699	−1.429
74	20	26.2	−1.301	−1.418
75	10	19.0	−1.000	−1.279
76	20	11.0	−1.301	−1.042
77	50	27.4	−1.699	−1.438
78	20	27.4	−1.301	−1.438
79	200	107.5	−2.301	−2.032
80	50	42.8	−1.699	−1.631
81	100	64.9	−2.000	−1.812
82	200	175.3	−2.301	−2.244

Multiple Linear Regression with Pseudoguaianolides and Eudesmanolides. The groups of the SLs from the pseudoguaianolide and from the eudesmanolide type consist of only 9 and 10 members, respectively, and are too small to draw final structure−activity relationships, but they were analyzed for the sake of completeness. The two hypocretenolides **92** and **93** are not separately observed and are only integrated into the entire dataset of 103 SLs.

QSAR analysis of the 9 pseudoguaianolides (for structures see Figure 8) yielded the following preliminary QSAR equation with two describing parameters which are statistically significant:

$$pIC_{100} = 0.984\ (\pm 0.097)\ \mathrm{UNC} - 1.233\ (\pm 0.286)\ \mathrm{HOM} - 26.574\ (\pm 3.052)$$

$$n = 9, R = 0.975, R^2 = 0.950, \mathrm{s} = 0.128, \mathrm{F} = 57.30, P = 0.0001 \quad (6)$$

Again, the number of unsaturated carbonyl groups is the most important parameter for the biological activity. Interestingly, this time the highest unoccupied molecular orbital (HOMO) is also involved in the structure−activity relationship of pseudoguaianolides.

For the 11 eudesmanolides (for structures see Figure 10), the following prelimary QSAR equation with three describing parameters was derived:

$$pIC_{100} = -1.067\ (\pm 0.325)\ \mathrm{SH1} + 1.862\ (\pm 0.531)\ \mathrm{SH2} + 0.804\ (\pm 0.286)\ \mathrm{ATOM} + 1.195\ (\pm 1.153)$$

$$n = 10, R = 0.860, R^2 = 0.740, s = 0.145, F = 5.70, P = 0.0343 \quad (7)$$

Eudesmanolides possess two six-membered rings and belong to the most rigid structures in the class of SLs. Consequently, the structure and shape coding parameters (SH1 and SH2) are most important for the description of the biological activity of this subgroup. The topological κ-shape descriptors according to Hall and Kier [24] describe different steric attributes of the molecule: whereas shape1 is related to the complexity or more precisely the cyclicity of the molecule, shape2 encodes information about the spatial density of atoms in a molecule. Up to now the studied eudesmanolides have inhibited NFκB DNA binding mostly at concentrations between 100 and 300 μM. Only SL **102** from *Mikania cordifolia* was more active with an IC_{100} value of 50 μM. More eudesmanolides should be investigated before final structure−activity relationships can be drawn.

Discussion

Sesquiterpene lactones have been the object of structure−activity relationship studies since the first examinations for their antiinflammatory and cytotoxic activity have been carried out.[2,25] Up to now the aim of these SAR or QSAR analysis has been to provide some insight into what structural features are related to these biological activities. Already in 1971 Kupchan et al. investigated a group of 26 SLs for their cytotoxicity on a human nasopharynx carcinoma cell line. They concluded, that the existence of an α-methylene-γ-lactone moiety is essential for their cytotoxic activity and that an α,β-unsaturated ester or cyclopentenone in the molecule strengthens this property. Cytotoxicity of bifunctional compounds, with two α,β-unsaturated carbonyl structural elements, did not correlate with lipophilicity, in contrast to monofunctional SLs whose activity increased with increasing log P.[25] Attempts to find a direct correlation between the rate of cysteine addition and cytotoxicity were unsuccessful, but the authors pointed out that a neighboring OH or O-acyl group enhances the rate of cysteine addition. In continuation of these investigations Schmidt untertook a QSAR study on cytotoxicity of a series of 21 pseudoguaianolide-type SLs in a murine Ehrlich Aszites tumor cell line and could confirm that cytotoxicity of SLs is strongly dependent on the number and type of alkylating centers. The molecular conformation and the number of H-bond acceptors, but not their position, turned out to be further deciding factors. The latter parameter indicates that noncovalent interactions of the SLs with proteins preceding alkylation may be important.[22] The correlation of the cytotoxic activity of 40 SLs toward a human cervix carcinoma cell line ameliorated when considering fractional accessible molecular surface areas (Q_frASAs) as describing parameters.[26] These studies underline that reactivity toward cysteine as well as

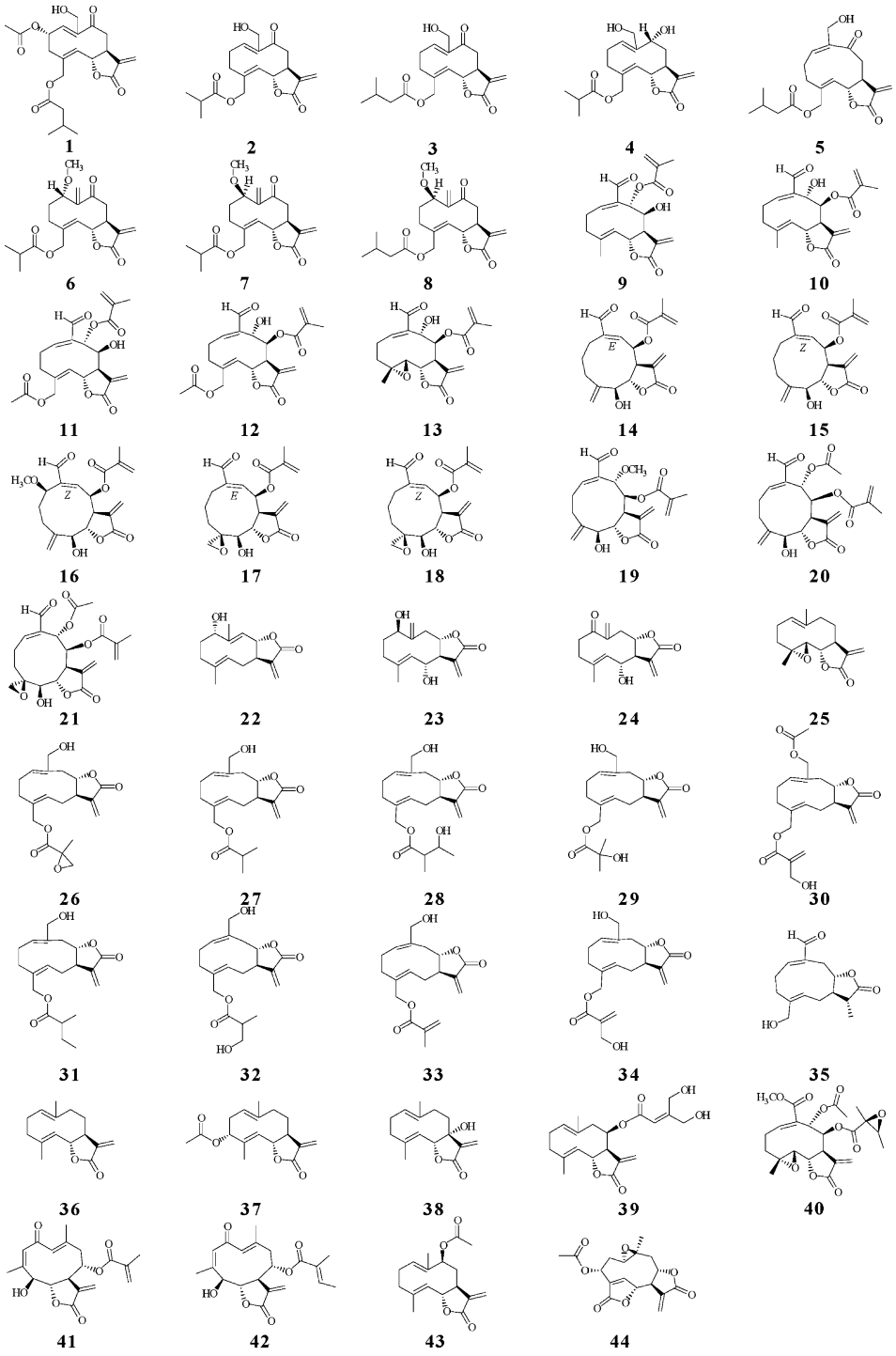

Figure 5. Structures of the investigated germacranolides.

interactions with further amino acids are important for their cytotoxic activity.

Additionally, cytoprotective activity was shown for SLs and it was presumed that SLs react as nucleophiles with SH-groups of the gastric mucosa in mice and protect them from ulcerations induced by necrotizing agents. The presence and the adequate molecular accessibility of an α,β-unsaturated carbonyl structural element and it's inclusion in a ring system or at least in the proximity of a cyclic system were established as essential factors.[27,28]

Preliminary comparative molecular field analysis (CoMFA) studies revealed that the activity of the SL parthenolide and its analogues in inhibiting serotonin release from blood platelets most likely involves both covalent binding and noncovalent interactions with the target molecule. The presence of an α-methylene-γ-lactone is not sufficient for inhibition of serotonin release.[29] Notably, a concave hydrophilic region adjacent to the lactone and a convex hydrophobic region on theopposite side of the molecule were important for interactions with the yet unidentified target molecule. Nevertheless, there are also some studies showing that the presence of an α-methylene-γ-lactone group is not a prerequisite for SL biological activities. It has been shown that SLs remarkably inhibit elastase release from granulocytes without possessing an α-methylene-γ-lactone moiety.[1]

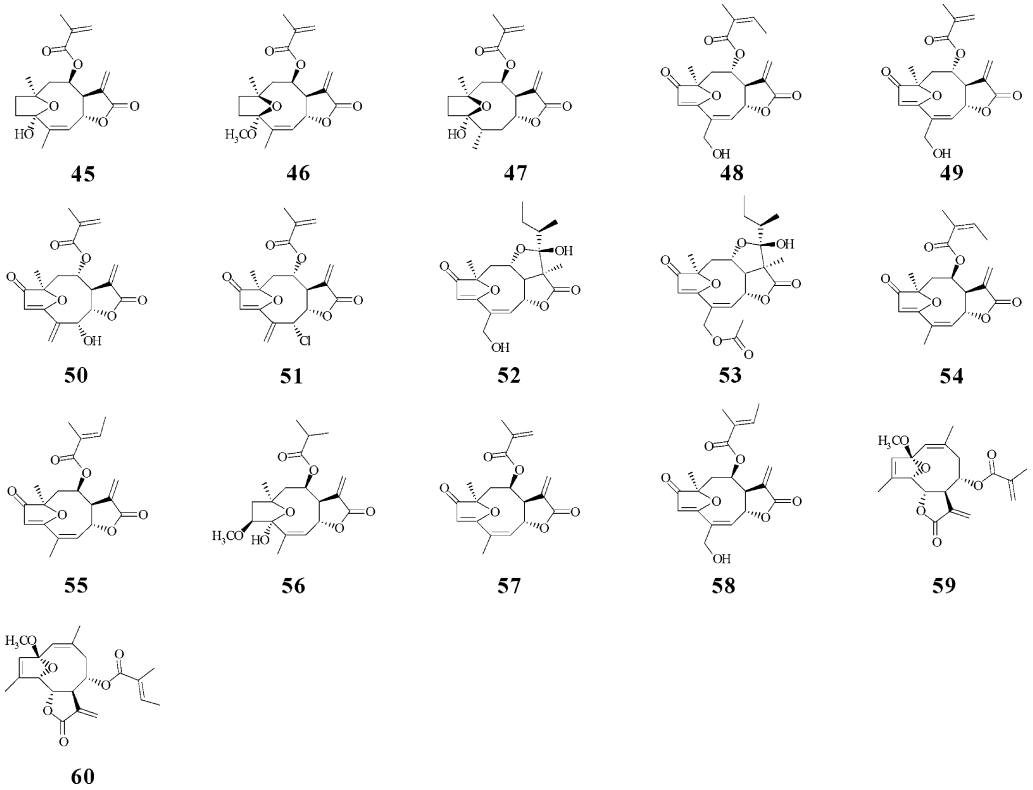

Figure 6. Structures of the investigated germacranolides subtype furanoheliangolides.

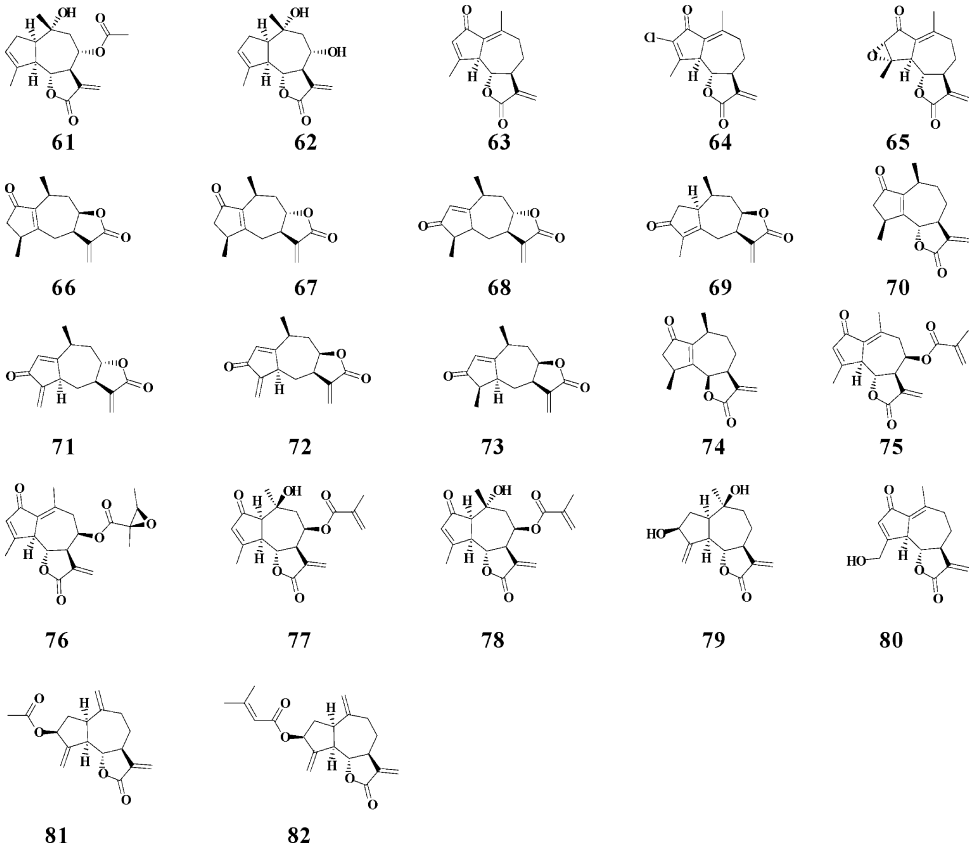

Figure 7. Structures of the investigated guaianolides.

Concerning the antiinflammatory activity proven in the carrageenan-induced edema in rats, previous structure−activity relationship studies revealed the α-methylene-γ-lactone moiety as the most decisive feature.[2]

Regarding the variety of structure−activity relationship studies with this class of natural compounds it is an interesting task to enhance our knowledge about the structural requirements for their various biological activities. Here, their antiinflammatory activity is of

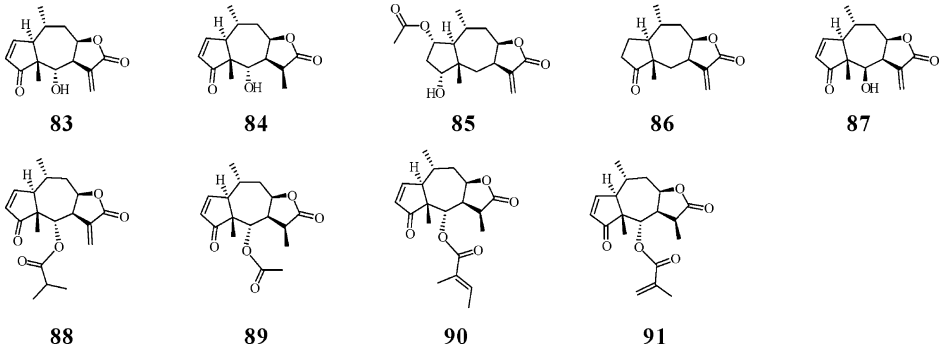

Figure 8. Structures of the investigated pseudoguaianolides.

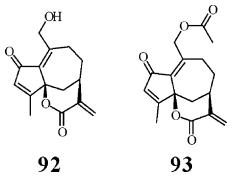

Figure 9. Structures of the investigated hypocretenolides.

major medicinal interest. Recently, we demonstrated that SLs inhibit DNA binding of the transcription factor NF-kB which could have beneficial effects in inflammation.[5,18,19] Therefore, we continued with our QSAR studies concerning the NF-κB inhibitory activity of SLs in an in vitro assay[9] and investigated a large set of 103 SLs.

The monoparametric regression of this total data set with all calculated parameters did not show any satisfactory solution. The best monoparametric correlation with $r = 0.68$ was obtained with the number of α,β-unsaturated carbonyl functions and was in accordance with our previous study with the data set of 28 SLs.[9] The low correlation coefficient could be due to great structural diversity of the used SLs.

On the basis of the multiple linear regression eq 1 for all 103 SLs, we can affirm that besides the number of α,β-unsaturated carbonyl functions, the occurrence of an α-methylene-γ-lactone moiety is the most important parameter for NF-κB inhibition, as already postulated by Rüngeler et al. for this test system.[9] Additionally, we could show that electron affinity and shape index3 are also important descriptors.

The unsaturated lactone moiety has already been proven to be an important, but sometimes not a sufficient, structural element for many biological activities of SLs, e.g. their antiinflammatory activity and cytotoxicity.[2,25] It has been discussed that these α,β-unsaturated structural elements react with nucleophils, such as thiol groups, in a Michael type addition.[30] Consequently, it is not surprising that the electron affinity, which correlates to the reactivity of the most reactive α,β-unsaturated carbonyl structure, is also an important descriptor. The fourth parameter, the shape index3, considers the molecule's centrality of branching and suggests that the molecular geometry as well as the occurrence and position of functional groups may have some impact on the activity. Recently, it was found that the analogous Kier and Hall index3 is important for the inhibition of the NF-κB-mediated gene expression by ethyl pyrimidinecarboxylates (EPC),[31] indicating that a certain shape is required for an efficient NF-κB inhibition.

Our results show that a selection of a lead compound from the total class of these structurally heterogeneous natural compounds is not possible. Therefore, we carried out QSAR analyses from the respective subgroups in which SLs can be divided according to the skeletal type.

In the group of germacranolides, similar parameters turned out to be important for the inhibitory activity as for the whole dataset of 103 SLs. This could be on one hand due to the fact that germacranolides provide the largest group among the investigated SLs. However, in contrast to eq 1 the topological parameter shape3 did not show a significant influence when only the germacranolides are considered. This could be explained by the relatively high flexibility of this subgroup. Due to their flexibility, they could easily adapt to the surrounding environment and the parameters quantifying the 3D structure would not be essential for activity. Equation 2 explains the heliangolide subgroup poorly. When the heliangolides are removed and the regression is recalculated, the correlation improves significantly. Here, either the number of unsaturated carbonyl functions or the existence of α,β-unsaturated acyl residues contribute to the NF-κB inhibitory activity.

The importance of α,β-unsaturated acyl residues for the activity contrasts with our previous study, where this feature did not significantly contribute to the inhibitory activity.[9] A possible explanation would be that α,β-unsaturated acyl residues could facilitate the reaction of SLs with the NF-κB protein by forming hydrogen bonds with the protein, stabilizing the covalent binding. Therefore, not only the existence but also the position of the acyl residues with respect to the methylene lactone could be of importance. However, Schmidt reported for the cytotoxic activity of SLs that only the number of H-bond acceptors, but not the position of such structure elements, is important.[22] Therefore, studies are in progress to clarify the importance of this parameter for the biological activity of SLs.

SLs in the subgroup of heliangolides have a much more rigid skeleton than the rest of the germacranolides. Consequently other structure-coding parameters are more important in the QSAR equation. Interestingly, the parameter ENONE (= existence of α,β-unsaturated carbonyl functions integrated in a ring system) seems to be more important than the α-methylene-γ-lactone function. Accordingly, SLs **46**, **47** and **56** only show a weak inhibitory activity despite of their α-methylene-γ-lactone, and SL **53**, missing this structural element, is active at a low concentration. Interestingly, heliangolides (**48**, **49**, **50**, **51**, **52**, **53**, **54**, **55**, **57**, **58**) which possessed an α,β,γ,δ-unsaturated carbonyl

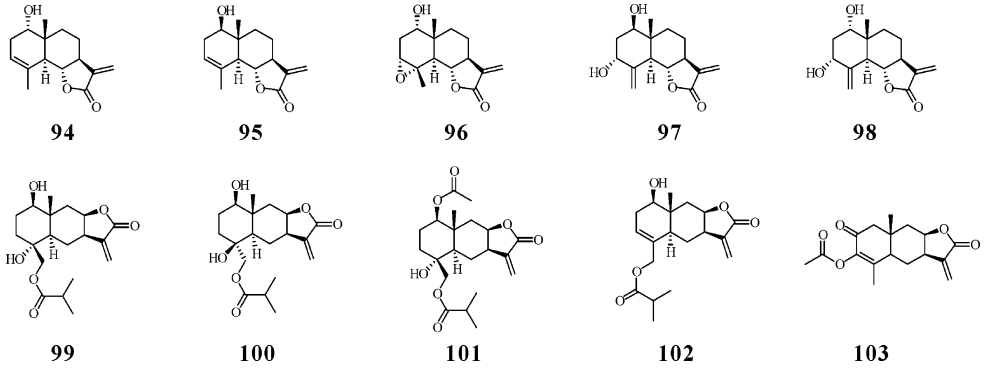

Figure 10. Structures of the investigated eudesmanolides.

Table 4. The Calculated Descriptors and the Abbreviation Used for the Calculations

Structural descriptor	Abbreviation
Total number of α,β-unsaturated carbonyl structures in the molecule (sum of ML, ENON and ACYL)	UNC
α-methylene-γ-lactone	ML
Conjugated ester groups	UNA
Conjugated keto or aldehyde functions	ENONE
Number of oxygen atoms	ATOM
Number of hydroxyl groups	OH
Octanol water partition coefficient	LOGP
Electron affinity[35]	EA
Dipole moment[35]	DIPOL
Molar refractivity[36]	MR
Connectivity Indices[24,37]	CN0-2
Shape Indices[24]	SH1-3
Highest occupied molecular orbital[35]	HOMO
Lowest unoccupied molecular orbitals[35]	LUMO1-3

system (= ENONE parameter) in addition to the unsaturated lactone inhibit NF-κB DNA binding at very low concentrations. The moderate inhibitory activity of SL **45** compared to SL **46** cannot be satisfactorily explained by the calculated equation. However, the hemiketal in SL **45** may be quite unstable and be rearranged to an α,β-unsaturated ketone which exhibits a high reactivity. This possibility is blocked by methylation of the free hydroxyl group in the case of SL **46** resulting in a higher IC_{100} value.

Guaianolides also possess a rigid skeleton. Accordingly, the NF-κB inhibitory activity is not only correlated to the number of unsaturated carbonyl structures in the molecule, but mostly to structure-coding parameters. Additionally, an increasing number of free hydroxyl groups diminishes the inhibitory activity. This is in agreement with other investigations suggesting the existence of an optimal number of hydroxyl groups for SL activity.[32] A lower number of hydroxyl groups correlates with a higher lipophilicity followed by a better penetration through cell membranes. Whether lipophilicity, expressed as log *P*, significantly contributes to the inhibitory activity in our study, as shown for the cytotoxic activity,[25] is doubtful. The parameter log *P* did not occur as a significant descriptor in our QSAR studies, which confirms our previous analyses.[9] Therefore, the position rather than the number of hydroxyl groups might have a more important role, as already described in the QSAR study related to cytotoxicity and serotonin release.[25,29]

Within the small group of eudesmanolides, the activity is mainly influenced by the topological shape parameters and the number of oxygen atoms that can react as hydrogen bond donors or acceptors thus being able to stabilize a reaction with the protein.

Conclusions

SLs have been suggested to serve as lead compounds for the design of new antiinflammatory drugs.[33] We here present for the first time a QSAR study on the NF-κB DNA binding activity of a great variety of structually different SLs. Moreover, this is the first study in which compounds are investigated whose mode of action in the NF-κB cascade is known. Our study shows that multiple linear regression analysis using the total data set of 103 SLs did not provide an equation which would allow a satifactory quantitative prediction of the inhibitory activity of new compounds. Consequently, it may also be unfavorable to select a lead compound considering all skeleton classes. Better insights into which structural features are related to the inhibitory activity and better correlation coefficients were obtained when subgroups of SLs, such as the furanoheliangolides, the germacranolides (excluding the furanoheliangolides) and guaianolides were used. Our QSAR studies indicate that topological and structure-coding parameters contribute to the NF-κB inhibitory activity of SLs possessing a rigid skeleton (furanoheliangolides and guaianolides), whereas in the case of flexible skeletons (germacranolides, such as germacrolides and melampolides), inhibition might be mostly determined by reactivity-coding parameters, such as the number and type of α,β-unsaturated carbonyl structural elements. When deciding to synthesize an NF-κB-inhibiting compound derived from a sesquiterpenoidal lead structure, a guaianolide, similar to SL **75** or **76**, would be mostly favorable for reasons of easier synthesis compared to a germacranolide or furanoheliangolide. The compound should possess two α,β-unsaturated carbonyl groups and an acyl moiety near the exocylic methylene group. Moreover, it has to be considered that the QSAR studies revealed here and in previous studies[2,3,9] correlate mostly with the structure−activity requirements for cytotoxicity.[22,25] Therefore, it is highly unlikely to separate the wanted therapeutic effects from the unwanted side effects such as cytotoxicity. This is also valid for the allergenicity.[34] To avoid this problem SLs could be either applied only externally, or they could be designed as a prodrug that would be liberated at the location of inflammation for the treatment of chronic inflammatory diseases.

Table 5. List of the Investigated SLs, Their Inhibitory Concentration (μM) in the NF-κB DNA Binding Assay and Their Origin

No.	Name	IC_{100}, μM	Origin
	I. Germacranolides		
	A. Germacranolides without Furanoheliangolides		
1	2α-Acetoxy-15-isovaleroyl-miguanin + 2α-Acetoxy-15-(2-methylbutyryl)-miguanin	12.5[9]	*Mikania guaco*[38]
2	15-Isobutyryl-miguanin	12.5	*M. guaco*[38]
3	15-Isovaleroyl-miguanin + 15-(2-Methylbutyryl)-miguanin	12.5	*M. guaco*[38]
4	9α,14-Dihydroxy-15-isobutyryloxy-costunolide	100	*M. guaco*[38]
5	14-Hydroxy-15-isovaleroyloxy-9-oxo-melampolide + 14-Hydroxy-15-(2-methylbutyryloxy)−9-oxo-melampolide	12.5[9]	*M. guaco*[38]
6	1α-Methoxy-15-isobutyryloxy-9-oxo-germacra-4*E*,10(14),11(13)-trien-12,6α-olide	25	*M. guaco*[38]
7	1β-Methoxy-15-isobutyryloxy-9-oxo-germacra-4*E*,10(14),11(13)-trien-12,6α-olide	25	*M. guaco*[38]
8	1β-Methoxy-15-isovaleroyloxy-9-oxo-germacra-4*E*,10(14),11(13)-trien-12,6α-olide + 1β-Methoxy-15-(2-methylbutyryloxy)−9-oxo-germacra-4*E*,10(14),11(13)-trien-12,6α-olide	12.5	*M. guaco*[38]
6	1α-Methoxy-15-isobutyryloxy-9-oxo-germacra-4*E*,10(14),11(13)-trien-12,6α-olide	25	*M. guaco*[38]
7	1β-Methoxy-15-isobutyryloxy-9-oxo-germacra-4*E*,10(14),11(13)-trien-12,6α-olide	25	*M. guaco*[38]
8	1β-Methoxy-15-isovaleroyloxy-9-oxo-germacra-4*E*,10(14),11(13)-trien-12,6α-olide + 1β-Methoxy-15-(2-methylbutyryloxy)−9-oxo-germacra-4*E*,10(14),11(13)-trien-12,6α-olide	12.5	*M. guaco*[38]
9	8β-Hydroxy-9α-methacryloyloxy-14-oxo-acanthospermolide	5[39]	*Milleria quinqueflora*[39]
10	9α-Hydroxy-8β-methacryloyloxy-14-oxo-acanthospermolide	10[39]	*M. quinqueflora*[39]
11	15-Acetoxy-9α-methacryloyloxy-8β-hydroxy-14-oxo-acanthospermolide	5[39]	*M. quinqueflora*[39]
12	15-Acetoxy-9α-hydroxy-8β-methacryl-oyloxy-14-oxo-acanthospermolide	5[39]	*M. quinqueflora*[39]
13	9α-Hydroxy-8β-methacryloyloxy-14-oxo-acanthospermolid-4α,5β-epoxide	10[39]	*M. quinqueflora*[39]
14	Miller-9*E*-enolide	5[39]	*M. quinqueflora*[39]
15	Miller-9*Z*-enolide	10[39]	*M. quinqueflora*[39]
16	1β-Methoxy-miller-9*Z*-enolide	10[9,39]	*M. quinqueflora*[39]
17	4β,15-Epoxy-miller-9*E*-enolide	5[9,39]	*M. quinqueflora*[39]
18	4β,15-Epoxy-miller-9*Z*-enolide	5[9,39]	*M. quinqueflora*[39]
19	9α-Methoxy-miller-1(10)*Z*-enolide	50[9,39]	*M. quinqueflora*[39]
20	9α-Acetoxy-miller-1(10)*Z*-enolide	10[9,39]	*M. quinqueflora*[39]
21	9α-Acetoxy-4β,15-epoxy-miller-1(10)*Z*-enolide	5[9,39]	*M. quinqueflora*[39]
22	Tatridin A	200	*Tanacetum praeteritum*[40c]
23	1-Epitatridin B	50	*T. praeteritum*[40c]
24	Tamirin	50[9]	*Tanacetum chiliophyllum*[41]
25	Parthenolide	20[9]	Aldrich
26	15-(2',3'-Epoxy)-isobutyryloxy-micrantholide	50	*Mikania cordifolia*[12]
27	15-Isobutyryloxy-micrantholide	50	*M. cordifolia*[12]
28	15-(2'-Methyl-3'-hydroxy)-butyryloxy-micrantholide	50	*M. cordifolia*[12]
29	15-(2'-Hydroxy)-isobutyryloxy-micrantholide	50	*M. cordifolia*[12]
30	14-Acetoxy-15-(3'-hydroxy)-methacryloyloxy-micrantholide	50	*M. cordifolia*[12]
31	15-(2'-Methyl)-butyryloxy-micrantholide	50	*M. cordifolia*[12]
32	15-(3'-Hydroxy)-isobutyryloxy-micrantholide	100	*M. cordifolia*[12]
33	15-Methacryloyloxy-micrantholide	50	*M. cordifolia*[12]
34	15-(4-Hydroxy)-methacryloyloxy-micrantholide	20	*M. cordifolia*[12]
35	11β,13-Dihydro-14-oxo-15-hydroxy-germacra-1(10)*E*,4*Z*-dien-12,8α-olide	300	*M. cordifolia*[12]
36	Costunolide	50[42]	*Podachaenium eminens*[42]
37	3-Acetoxy-costunolide	50[42]	*P. eminens*[42]
38	7-Hydroxy-costunolide	10[42]	*P. eminens*[42]
39	Eupatoriopikrin	20	*Eupatorium cannabinum*[a]
40	Enhydrine	10	*Smallanthus sonchifolius*[b]
41	Molephantin	10	*Elephantopus mollis*[43]
42	Molephantinin	10	*E. mollis*[43]
43	9β-Acetoxycostunolide	200	*Zinnia haageana*[44]
44	Scandenolide	10	*Mikania micrantha*[d]
	B. Furanoheliangolides		
45	Diversifolin	50[9,45]	*Tithonia diversifolia*[45]
46	Diversifolin-methyl ether	200[9,45]	*T. diversifolia*[45]
47	Tirotundin	200[9,45]	*T. diversifolia*[45]
48	Centratherin	5[9]	*Proteopsis furnensis*[46]
49	Goyazensolide	20[9]	*Eremanthus mattogrossensis*[47]
50	Isogoyazensolide	10[9]	*E. mattogrossensis*[47]
51	1-Oxo-5-chlor-3,10-epoxy-8-methacryloyloxy-germacra-2,4(15),11(13)-trien-12,6α-olide	5	Artifact from 42[47]
52	15-Hydroxy-eremantholide B	100[9]	*Eremanthus arboreus*[48]
53	15-Acetoxy-eremantholide B	5[9]	*E. arboreus*[48]
54	15-Deoxybudlein A	2.5−5	*Calea lantanoides*[49]
55	Atripliciolide tiglate	5	*Viguiera robusta*[50]
56	10-Hydroxy-2-methoxy-3,10-epoxy-8-(2-methylpropanoyl-oxy)-germacra-4,11(13)-dien-12,6α-olide	200	*Tithonia diversifolia*[51]
57	15-Deoxygoiazensolide	10	*Vanillomopsis erythropappa*[52b]
58	Budlein A	5	*Viguiera arenaria*[53]
59	2β-Methoxy-2-deethoxy-phantomolin	10	*Elephantopus mollis*[43]
60	2β-Methoxy-2-deethoxy-8-O-deacylphantomolin-8-O-tiglinate	10	*E. mollis*[43]

Table 5 (Continued)

No.	Name	IC_{100}, μM	Origin
	II. Guaianolides		
61	Cumambrin A	20[9]	*Tanacetum densum*[54]
62	Cumambrin B	100[9]	*T. densum*[54]
63	Dehydro-leucodin	50[42]	*Podachaenium eminens*[42]
64	3-Chloro-dehydroleucodin	20[42]	*P. eminens*[42]
65	3,4-Epoxy-dehydroleucodin	5[42]	*P. eminens*[42]
66	2-Oxo-guaia-1(5),11(13)-dien-12,8β-olide	20	*Decachaeta thieleana*[e]
67	2-Oxo-guaia-1(5),11(13)-dien-12,8α-olide	20	*D. thieleana*[e]
68	Thieleanin	20	*D. thieleana*[e]
69	3-Oxo-guaia-4,11(13)-dien-12,8β-olide	50	*D. thieleana*[e]
70	2-Oxo-guaia-1(5),11(13)-dien-12,6β-olide	20	*D. thieleana*[e]
71	3-Oxo-guaia-1,4(15), 11(13)-trien-12,8β-olide	5	*D. thieleana*[e]
72	3-Oxo-guaia-1,4,11(13)-trien-12,8α-olide	10	*D. thieleana*[e]
73	3-Oxo-guaia-1(2),11(13)-dien-12,8α-olide	50	*D. thieleana*[e]
74	2-Oxo-guaia-1(5),11(13)-dien-12,6α-olide	20	*D. thieleana*[e]
75	2-Oxo-8β-methacryloyloxy-guaia-1(10),3,11(13)-trien-12,6α-olide	10[55]	*Viguiera gardneri*[55]
76	2-Oxo-8β-epoxyangelicoyloxy-guaia-1(10),3,11(13)-trien-12,6α-olide	20	*V. grandiflora*[b]
77	2-Oxo-8β-methacryloyloxy-10β-hydroxy-guaia-3,11 (13)-dien-12,6α-olide	50[55]	*V. gardneri*[55]
78	2-Oxo-8β-methacryloyloxy-10α-hydroxy-guaia-3,11 (13)-dien-12,6α-olide	20[55]	*V. gardneri*[55]
79	3β,10α-Dihydoxy-guaia-4(15),11(13)-dien-12,6α-olide	200	*Picris altissima*[56]
80	2-Oxo-15-hydroxy-guaia-1(10),3,11(13)-trien-12,6α-olide	50	*Cichorium intybus*[57]
81	3β-Acetoxy-guaia-4(15),10(14),11(13)-trien-12,6α-olide	100	*Vernonia flexuosa*[58]
82	3β-Senecioyloxy-guaia-4(15),10(14),11(13)-trien-12,6α-olide	200	*V. flexuosa*[58]
	III. Pseudoguaianolides		
83	Helenalin	10[9]	*Arnica chamissonis ssp. foliosa*[59]
84	11α,13-Dihydrohelenalin	200[9]	*A. chamissonis ssp. foliosa* [59]
85	Chamissonolide	200[9]	*A. chamissonis ssp. foliosa* [59]
86	2,3-Dihydroaromaticin	50[9]	*Arnica cordifolia*[60]
87	Mexicanin I	20[9]	*Arnica acaulis*[61]
88	Helenalinisobutyrate	20[9]	*A. chamissonis ssp. foliosa*[59]
89	11α,13-Dihydrohelenalinacetate	200[5]	*A. montana*[5]
90	11α,13-Dihydrohelenalintiglinate	100[5]	*A. montana*[5]
91	11α,13-Dihydrohelenalinmethacrylate	100[5]	*A. montana*[5]
	IV. Hypocretenolides		
92	14-Hydroxy-hypocretenolide	50[62]	*Leontodon hispidus*[62]
93	14-Acetoxy-hypocretenolide	100	*Crepis aurea*[63]
	V. Eudesmanolides		
94	Douglanin	300	*Tanacetum praeteritum*[64c]
95	Santamarin	100[9]	*T. praeteritum*[64]
96	Ludovicin A	200	*T. praeteritum*[64c]
97	3α-Hydroxyreynosin	200[9]	*T. praeteritum*[64]
98	Ludovicin B	100	*T. praeteritum*[64c]
99	1β,4α-Dihydroxy-15-isobutyryloxy-eudesma-11(13)-en-12,8β-olide	200	*M. cordifolia*[12]
100	1β,4β-Dihydroxy-15-isobutyryloxy-eudesma-11(13)-en-12,8β-olide	200	*M. cordifolia*[12]
101	1β-Acetoxy-4α-hydroxy-15-isobutyryloxy-eudesma-11(13)-en-12,8β-olide	100	*M. cordifolia*[12]
102	1β-Hydroxy-15-isobutyryloxy-eudesma-3,11(13)-dien-12,8β-olide	50	*M. cordifolia*[12]
103	2-Oxo-3-acetoxy-eudesma-3,11(13)-dien-12,8β-olide	100	*D. thieleana*[e]

[a] Kindly provided by Prof. Becker, Universität Saarbrücken, Germany. [b] Da Costa et al., unpublished results. [c] Kindly provided by Prof. N. Gören, Marmara Research Center, Gebze-Kocaeli, Turkey. [d] Isolation;[65] identification.[66] [e] R. Murillo, V. Castro, A. J. García-Piñeres, C. A. Klaas, I. Merfort. Unpublished results.

Experimental Section

Test Compounds. The 103 SLs were isolated from different Asteraceae species as listed in Table 5. Stock solutions (10 mM) were prepared in DMSO for the NF-κB EMSAs. The structures of the investigated SLs are shown in Figures 5−10. Purity was evaluated by GC or HPLC analysis and was >98%, respectively.

Cell Culture. Jurkat T-Cells were maintained in RPMI 1640 medium supplemented with 10% fetal calf serum, 100 IU/mL penicillin and 100 μg/mL streptomycin (all from Life Technologies, Inc.).

NF-κB Electrophoretic Mobility Shift Assay (EMSA). Jurkat T-cells were incubated for 1 h and subsequently stimulated with TNF-α for 1 h. Total protein extracts were prepared and analyzed for NF-κB binding activity in an electrophoretic mobility shift assay (EMSA). All experiments were reproduced at least once. Total cell extracts from Jurkat T-cells were prepared using a high salt detergent buffer (Totex: 20 mM Hepes pH 7.9, 0.5 mM EDTA, 0.1 mM EGTA, 0.5 mM DTT, 0.1% phenylmethylsulfonyl fluoride, 1% aprotinin). Cells were harvested by centrifugation, washed once in ice-cold phosphate-buffered saline (PBS, Sigma), and resuspended in 4 cell volumes of Totex buffer. The cell lysate was incubated on ice for 30 min and then centrifuged for 5 min at 13 000 rpm at 4 °C. The protein content of the supernatant was determined, and equal amounts of protein (10−20 μg) were added to a reaction mixture containing 20 μg of bovine serum albumin (Sigma), 2 μg of poly (dI-dC) (Roche Molecular Biochemicals, 2 μL of buffer D+ (20 mM Hepes pH 7.9, 20% glycerol, 100 mM KCl, 0.5 mM EDTA, 0.25% Nonidet P-40, 2 mM DTT, 0.1% phenylmethylsulfonyl fluoride), 4 μL of buffer F (20% Ficoll 400, 100 mM Hepes, 300 mM KCl, 10 mM DTT, 0.1% phenylmethylsulfonyl fluoride) and 100 000 cpm (Cerenkov) of a ^{32}P-labeled oligonucleotide made up to a final volume of 20 μL with distilled water. Samples were incubated at room temperature for 25 min. NF-κB oligonucleotide (Promega) was labeled using [γ^{32}P]dATP (3000 Ci/mmol; Amersham Pharmacia Biotech) and a T4 polynucleotide kinase (New England Biolabs).

Data Set. The biological activity of SLs is expressed as the μM concentration which totally blocked the DNA-binding of

the transcription factor NF-κB in the EMSA, here called IC_{100}. In the calculations pIC_{100} (corresponding to $-\log IC_{100}$) are used.

Descriptor Calculation. The three-dimensional structures of the molecules were created using the molecular modeling package HyperchemPro (Version 6.02). Energy minimizations were performed with the force field MM+ using the Polak-Ribière minimization algorithm. Low energy conformations of the SLs were created using the conformational search option. The starting structures were initially minimized to an RMS gradient <0.01 kcal mol^{-1} $Å^{-1}$. All rotatable cyclic bonds were included as variable torsions and allowed to be changed simultaneously. The search was performed applying a usage-directed search method and standard settings for duplication test. A search run was terminated after energy minimization of 2500 unique starting geometries. Acyl side chains were not included in the conformational search. They were added manually to the SL-conformer with the lowest energy, and the resulting models were energy minimized to an RMS-gradient as described above. The final geometries were obtained with the semiempirical AM1 method. The resulting geometries were transferred to the software CAChe (Fujitsu Inc.), which can calculate constitutional, topological, electrostatic and quantum chemical descriptors. Constitutional descriptors are related to the number of atoms, bonds and functional groups in each molecule. Topological descriptors, like the shape and connectivity indices, include valence and nonvalence molecular connectivity indices calculated from the hydrogen suppressed formula of the molecule, encoding about the size, composition and the degree of branching in the molecule. The quantum chemical descriptors include information about the molecular orbital energy levels. For all calculated descriptors and their abbreviations used in the following calculations, see Table 4.

Model Selection by Means of Multiple Linear Regression. After calculation of the descriptors, an intercorrelation analysis of the descriptors was performed. During the regression analysis, equations containing variables with an intercorrelation coefficient >0.85 were discarded. Selection of relevant descriptors was performed using the SAS.6.12 Procedure REG (SAS Institute Inc., Cary, NC; REG = multiple linear regression). However, we did not make use of one of the built-in selection criteria like "forward" or "backward" but proceeded in the following way: At first we calculated the best correlation (with the highest R^2 as a measure of explained variation) from one up to five descriptors. All descriptors were included in each calculation, respectively. For discussion we selected the equation with the highest R^2 and in which all descriptors contributed significantly to the model fit.

Acknowledgment. We gratefully acknowledge financial support from the VolkswagenStiftung.

References

(1) Siedle, B.; Gustavsson, L.; Johansson, S.; Murillo, R.; Castro, V.; Bohlin, L.; Merfort, I. The effect of sesquiterpene lactones on the release of human neutrophil elastase. *Biochem. Pharmacol.* **2003**, *65*, 897−903.

(2) Hall, I. H.; Lee, K. H.; Starnes, C. O.; Sumida, Y.; Wu, R. Y.; Waddell, T. G.; Cochran, J. W.; Gerhart, K. G. Antiinflammatory activity of sesquiterpene lactones and related compounds. *J. Pharm. Sci.* **1979**, *68*, 537−541.

(3) Hall, I. H.; Starnes, C. O., Jr.; Lee, K. H.; Waddell, T. G. Mode of action of sesquiterpene lactones as antiinflammatory agents. *J. Pharm. Sci.* **1980**, *69*, 537−543.

(4) Willuhn, G. *Arnica* flowers: pharmacology, toxicology, and analysis of the sesquiterpene lactones−their main active substances. In *Phytomedicines of Europe: Chemistry and Biological Activity;* Lawson, L. D., Bauer, R., Eds.; American Chemical Society: Washington, DC, 1998; pp 118−132.

(5) Klaas, C. A.; Wagner, G.; Laufer, S.; Sosa, S.; Della Loggia, R.; Bomme, U.; Pahl, H. L.; Merfort, I. Studies on the anti-inflammatory activity of phytopharmaceuticals prepared from Arnica flowers. *Planta Med.* **2002**, *68*, 385−391.

(6) Tornhamre, S.; Schmidt, T. J.; Nasman-Glaser, B.; Ericsson, I.; Lindgren, J. A. Inhibitory effects of helenalin and related compounds on 5-lipoxygenase and leukotriene C(4) synthase in human blood cells. *Biochem. Pharmacol.* **2001**, *62*, 903−911.

(7) Dirsch, V. M.; Stuppner, H.; Vollmar, A. M. Helenalin triggers a CD95 death receptor-independent apoptosis that is not affected by overexpression of Bcl-x(L) or Bcl-2. *Cancer Res.* **2001**, *61*, 5817−5823.

(8) Lyss, G.; Schmidt, T. J.; Merfort, I.; Pahl, H. L. Helenalin, an anti-inflammatory sesquiterpene lactone from Arnica, selectively inhibits transcription factor NF-κB. *Biol. Chem.* **1997**, *378*, 951−961.

(9) Rüngeler, P.; Castro, V.; Mora, G.; Goren, N.; Vichnewski, W.; Pahl, H. L.; Merfort, I.; Schmidt, T. J. Inhibition of transcription factor NF-κB by sesquiterpene lactones: a proposed molecular mechanism of action. *Bioorg. Med. Chem.* **1999**, *7*, 2343−2352.

(10) Wong, H. R.; Menendez, I. Y. Sesquiterpene lactones inhibit inducible nitric oxide synthase gene expression in cultured rat aortic smooth muscle cells. *Biochem. Biophys. Res. Commun.* **1999**, *262*, 375−380.

(11) Bork, P. M.; Schmitz, M. L.; Kuhnt, M.; Escher, C.; Heinrich, M. Sesquiterpene lactone containing Mexican Indian medicinal plants and pure sesquiterpene lactones as potent inhibitors of transcription factor NF-kappaB. *FEBS Lett.* **1997**, *402*, 85−90.

(12) Klaas, C. A. Phytochemische und pharmakologisch-biologische Untersuchungen von *Mikania cordifolia* sowie Studien zum molekularen Wirkmechanismus von Sesquiterpenlactonen unter Verwendung des Transkriptionsfaktors NF-AT. Thesis, University Freiburg, 2001.

(13) Kuklina, E. M.; Shirshev, S. V. Role of transcription factor NFAT in the immune response. *Biochemistry (Moscov)* **2001**, *66*, 467−475.

(14) Lee, J. I.; Burckart, G. J. Nuclear factor kappa B: important transcription factor and therapeutic target. *J. Clin. Pharmacol.* **1998**, *38*, 981−993.

(15) Baeuerle, P. A.; Henkel, T. Function and activation of NF−B in the immune system. *Annu Rev Immunol* **1994**, *12*, 141−179.

(16) Pahl, H. L. Activators and target genes of Rel/NF-κB transcription factors. *Oncogene* **1999**, *18*, 6853−6866.

(17) Barnes, P. J.; Karin, M. Nuclear factor-kappaB: a pivotal transcription factor in chronic inflammatory diseases. *N. Engl. J. Med.* **1997**, *336*, 1066−1071.

(18) Lyss, G.; Knorre, A.; Schmidt, T. J.; Pahl, H. L.; Merfort, I. The anti-inflammatory sesquiterpene lactone helenalin inhibits the transcription factor NF-κB by directly targeting p65. *J. Biol. Chem.* **1998**, *273*, 33508−33516.

(19) Garcia-Pineres, A. J.; Castro, V.; Mora, G.; Schmidt, T. J.; Strunck, E.; Pahl, H. L.; Merfort, I. Cysteine 38 in p65/NF-kappaB plays a crucial role in DNA binding inhibition by sesquiterpene lactones. *J. Biol. Chem.* **2001**, *276*, 39713−39720.

(20) Kupchan, S. M.; Fessler, D. C.; Eakin, M. A.; Giacobbe, T. Reaction of alpha methylene lactone tumor inhibitors with model biological nucleophiles. *Science* **1970**, *168*, 376−379.

(21) Schmidt, T. J. Helenanolide-type sesquiterpene lactones- III. Rates and stereochemistry in the reaction of helenalin and related helenanolides with sulfhydryl containing biomolecules. *Bioorg. Med. Chem.* **1997**, *5*, 645−653.

(22) Schmidt, T. J. Quantitative structure-cytotoxicity relationships within a series of helenanolide type sesquiterpene lactones. *Pharm. Pharmacol. Lett.* **1999**, *9*, 9−13.

(23) Fischer, N. H. Sesquiterpenoid lactones. In *Methods in plant biochemistry;* Charlwood, B. V., Banthorpe, D. V., Eds.; Academic Press limited: London, 1991; pp 187−211.

(24) Hall, L. H.; Kier, L. B. The molecular connectivity chi indexes and kappa shape indexes in structure−property modeling. In *Reviews in Computational Chemistry*; Lipkowitz, K. B., Boyd, D. B., Eds.; 1992; pp 367−422.

(25) Kupchan, S. M.; Eakin, M. A.; Thomas, A. M. Tumor inhibitors. 69. Structure-cytotoxicity relationships among the sesquiterpene lactones. *J. Med. Chem.* **1971**, *14*, 1147−1152.

(26) Schmidt, T. J.; Heilmann, J. Quantitative structure-cytotoxicity relationships of sesquiterpene lactones derived from partial charge (Q)-based fractional accessible surface area descriptors (Q_frASAs). *Quant. Struct.−Act. Relat.* **2002**, *21*, 276−287.

(27) Rodriguez, A. M.; Enriz, R. D.; Santagata, L. N.; Jauregui, E. A.; Pestchanker, M. J.; Giordano, O. S. Structure-cytoprotective activity relationship of simple molecules containing an α,β-unsaturated carbonyl system. *J. Med. Chem.* **1997**, *40*, 1827−1834.

(28) Enriz, R. D.; Rodriguez, A. M.; Jauregui, E. A.; Pestchanker, M. J.; Giordano, O. S.; Guzman, J. Structure−activity relationship in the cytoprotective effect of helenalin and related compounds. *Drug Des. Discovery* **1994**, *11*, 23−38.

(29) Marles, R. J.; Pazos-Sanou, L.; Compadre, C. M.; Pezzuto, J. M.; Bloszyk, E.; Arnason, J. T. Sesquiterpene lactones revisited. In *Phytochemistry of Medicinal Plants*; Arnason, J. T., Ed.; Plenum Press: New York, 1995; pp 333−356.

(30) Schmidt, T. J. Toxic activities of sesquiterpene lactones: structural and biochemical aspects. *Curr. Org. Chem.* **1999**, *3*, 577−608.

(31) Liu, H. X.; Zhang, R. S.; Yao, X. J.; Liu, M. C.; Hu, Z. D.; Fan, B. T. QSAR study of ethyl 2-[(3-methyl-2,5-dioxo(3-pyrrolinyl))-amino]-4-(trifluoromethyl) pyrimidine-5-carboxylate: an inhibitor of AP-1 and NF-kappa B mediated gene expression based on support vector machines. *J. Chem. Inf. Comput. Sci.* **2003**, *43*, 1288−1296.
(32) Macias, F. A.; Galindo, J. C.; Castellano, D.; Velasco, R. F. Sesquiterpene lactones with potential use as natural herbicide models. 2. guaianolides. *J. Agric. Food Chem.* **2000**, *48*, 5288−5296.
(33) Willuhn, G. Sesquiterpenlactone, potentielle Leitsubstanzen für die Arzneistofffindung. *Dtsch. Apoth. Ztg.* **1987**, *127*, 2511−2517.
(34) Hausen, B. M.; Vieluf, I. K. *Allergiepflanzen−Pflanzenallergene: Handbuch und Atlas der allergie-induzierenden Wild- und Kulturpflanzen*; Ecomed Verlagsgesellschaft, 2001.
(35) Dewar, M. J. S.; Zoebisch, E. G.; Healy, E. F.; Stewart, J. J. P. AM1: A new general purpose quantum mechanical molecular model. *J. Am. Chem. Soc.* **1985**, *107*, 3902−3909.
(36) Ghose, A. K.; Pritchett, A.; Crippen, G. M. Atomic physicochemical parameters for three-dimensional structure-directed quantitative structure−activity relationships 3. *J. Comput. Chem.* **1988**, *9*, 80−90.
(37) Kier, L. B.; Hall, L. H. *Molecular Connectivity in Structure−Activity Analysis*; Research Studies Press: Wiley: Letchworth, England, 1986.
(38) Rüngeler, P.; Brecht, V.; Tamayo-Castillo, G.; Merfort, I. Germacranolides from Mikania guaco. *Phytochemistry* **2001**, *56*, 475−489.
(39) Castro, V.; Rüngeler, P.; Murillo, R.; Hernandez, E.; Mora, G.; Pahl, H. L.; Merfort, I. Study of sesquiterpene lactones from *Milleria quinqueflora* on their anti-inflammatory activity using the transcription factor NF-κB as molecular target. *Phytochemistry* **2000**, *53*, 257−263.
(40) Goren, N.; Woerdenbag, H. J.; Bozok-Johansson, C. Cytotoxic and antibacterial activities of sesquiterpene lactones isolated from *Tanacetum praeteritum subsp. praeteritum*. *Planta Med.* **1996**, *62*, 419−422.
(41) Goren, N.; Tahtasakal, E. Sesquiterpenes of *Tanacetum chiliophyllum var. heimerlei*. *Phytochemistry* **1993**, *34*, 1071−1073.
(42) Castro, V.; Murillo, R.; Klaas, C. A.; Meunier, C.; Mora, G.; Pahl, H. L.; Merfort, I. Inhibition of the transcription factor NF-kappa B by sesquiterpene lactones from *Podachaenium eminens*. *Planta Med.* **2000**, *66*, 591−595.
(43) Banerjee, S.; Schmeda-Hirschmann, G.; Castro, V.; Schuster, A.; Jakupovic, J.; Bohlmann, F. Further sesquiterpene lactones from *Elephantopus mollis* and *Centratherum punctatum*. *Planta Med.* **1986**, 29−32.
(44) Kisiel, W. A new germacranolide from *Zinnia haageana*. *Phytochemistry* **1978**, *17*, 1059−1060.
(45) Rüngeler, P.; Lyss, G.; Castro, V.; Mora, G.; Pahl, H. L.; Merfort, I. Study of three sesquiterpene lactones from *Tithonia diversifolia* on their antiinflammatory activity using the transcription factor NF-κB and enzymes of the arachidonic acid pathway as targets. *Planta Med.* **1998**, *64*, 588−593.
(46) Vichnewski, W.; Leitsaho Filho, H. F.; Nakashima, C.; Lunardello, M. A.; Gutierrez, A. B.; Herz, W. Centratherin and lychnopholide from a new *Proteopsis* species. *Rev. Latinoam. Quim.* **1990**, *21*, 28−29.
(47) Lunardello, M. A.; Tomaz, J. C.; Vichnewski, W.; Lopes, J. L. C. Sesquiterpene lactones and flavonoids from *Eremanthus mattogrossensis* and *Eremanthus eriopus*. *J. Braz. Chem. Soc.* **1995**, *6*, 307−311.
(48) Vichnewski, W.; Skrochy, C. A. T. T.; Nasi, A. M.; Calleagri Lopes, J. L.; Herz, W. 15-Hydroxyeremantholide B and derivatives from *Eremanthus arboreus*. *Phytochemistry* **1999**, *50*, 317−320.
(49) Vichnewski, W.; Goulart, E. G.; Herz, W. A heliangolide from *Calea lantanoides*. *Phytochemistry* **1982**, *21*, 464−465.
(50) Da Costa, F. B.; Vichnewski, W.; Herz, W. Constituents of *Viguiera aspillioides* and *V. robusta*. *Biochem. Syst. Ecol.* **1996**, *24*, 585−587.
(51) Pereira, P. S.; Dias, D. A.; Vichnewski, W.; Nasi, A. M.; Herz, W. Sesquiterpene lactones from Brazilian *Tithonia diversifolia*. *Phytochemistry* **1997**, *45*, 1445−1448.
(52) Vichnewski, W.; Lopes, J. L. C.; Dos Santos Filho, D.; Herz, W. 15-Deoxygoiazensolide, a new heliangolide from *Vanillomopsis erythropappa*. *Phytochemistry* **1976**, *15*, 1775−1776.
(53) Da Costa, F. B.; Ito, I. Y.; Andre, R. F. G.; Vichnewski, W. Constituents of *Viguiera* species with antibacterial activity. *Fitoterapia* **1998**, *69*, 86−87.
(54) Goren, N.; Bozok-Johansson, C.; Jakupovic, J.; Lin, L.-J.; Shieh, H.-L.; Cordell, G. A.; Celik, N. Sesquiterpene lactones with antibacterial activity from *Tanacetum densum ssp. sivasicum*. *Phytochemistry* **1992**, *31*, 101−104.
(55) Schorr, K.; Garcia-Pineres, A. J.; Siedle, B.; Merfort, I.; Da Costa, F. B. Guaianolides from *Viguiera gardneri* inhibit the transcription factor NF-κB. *Phytochemistry* **2002**, *60*, 733−740.
(56) Kisiel, W. Guaianolides from *Picris altissima*. *Phytochemistry* **1992**, *31*, 328−329.
(57) Kisiel, W.; Zielinska, K. Guaianolides from *Cichorium intybus* and structure revision of Cichorium sesquiterpene lactones. *Phytochemistry* **2001**, *57*, 523−527.
(58) Kisiel, W. Phytochemical investigation of *Vernonia flexuosa* Sims. Part II Vernoflexoside and vernoflexin−new sesquiterpenelactones. *Pol. J. Pharmacol. Pharm.* **1975**, *27*, 461−467.
(59) Willuhn, G.; Kresken, J.; Leven, W. Further helenanolides from the flowers of *Arnica chamissonis* ssp. *foliosa*. *Planta Medica* **1990**, *56*, 111−115.
(60) Merfort, I.; Wendisch, D. Sesquiterpene lactones of *Arnica cordifolia*. *Phytochemistry* **1993**, *34*, 1437.
(61) Leven, W. Qualitative und quantitative chromatographische (DC, GC, HPLC) und photometrische Analyse der Sesquiterpenlactone in "Arnikablüten DAB 9" und Untersuchungen zur Sesquiterpenlactonführung in Blüten von *Arnica acaulis*. Thesis, Universität Düsseldorf, 1988.
(62) Zidorn, C.; Dirsch, V. M.; Rüngeler, P.; Sosa, S.; Della Loggia, R.; Merfort, I.; Pahl, H. O.; Vollmar, A. M.; Stuppner, H. Antiinflammatory activities of hypocretenolides from *Leontodon hispidus. Planta Med.* **1999**, *65*, 704−708.
(63) Kisiel, W. Hypocretenolides from *Crepis aurea*. *Fitoterapia* **1994**, *65*, 381.
(64) Goren, N. Sesquiterpene lactones from *Tanacetum praeteritum*. *Phytochemistry* **1995**, *38*, 1261−1264.
(65) Siedle, B. Phytochemische und pharmakologisch-biologische Untersuchungen von traditionellen Heilpflanzen aus Costa Rica sowie von Sesquiterpenlactonen und Bindungs- und QSAR−Studien mit der Humanen Neutrophilen Elastase und dem Transkriptionsfaktor NF-κB als molekularen Targets. Thesis, Albert-Ludwigs Universität Freiburg, 2003.
(66) Cuenca, M. d. R.; Bardon, A.; Catalan, C. A. N. Sesquiterpene lactones from *Mikania micrantha*. *J. Nat. Prod.* **1988**, *51*, 625−626.

JM049937R